ACS SENSORS

pubs.acs.org/acssensors

Article

Label-Free, Novel Electrofluidic Capacitor Biosensor for Prostaglandin E2 Detection toward Early and Rapid Urinary Tract Infection Diagnosis

Antra Ganguly, Tahmineh Ebrahimzadeh, Philippe Zimmern, Nicole J. De Nisco, and Shalini Prasad*

Cite This: *ACS Sens.* 2022, 7, 186−198

Read Online

ACCESS | Metrics & More | Article Recommendations | Supporting Information

ABSTRACT: Urine Prostaglandin E2 (PGE2) has been identified as an attractive diagnostic and prognostic biomarker for urinary tract infection (UTI). This work demonstrates the use of PGE2 as a biomarker for rapid and label-free testing for UTI. In this work, we have developed a novel electrofluidic capacitor-based biosensor that can used for home-based UTI management with high accuracy in less than 5 min for small volume urine samples (<60 μL). The PGE2 biosensor works on the principle of affinity capture using highly specific monoclonal PGE2 antibody and relies on non-faradaic electrical impedance spectroscopy (EIS) and Mott−Schottky (MS) for quantifying subtle variations in PGE2 levels expressed in human urine (pH 5−8). Dynamic light scattering experiments were performed to characterize surface charge properties and the impact of bulk interferents on the interfacial modulation of electrical properties due to binding and urine pH variations. Binding chemistry between the key elements of the immunosensor stack was validated using attenuated total reflectance-Fourier transform infrared spectroscopy and surface plasmon resonance studies. Linear calibration dose responses were obtained for PGE2 for both EIS and MS. The sensor reliably distinguished between UTI negative and UTI positive cases for both artificial (pH 5−8) and pooled human urine samples. The sensor was not found to cross-react with Prostaglandin D2, a structurally similar interferent, and other abundant urine interferents (urea and creatinine). Human subject studies confirmed the validity of the sensor for robust and accurate UTI diagnosis. This work can be extended to achieve easy, reliable, and rapid home-based UTI management, which can consequently help physicians with timely and appropriate administration of therapy to improve patient outcomes and treatment success.

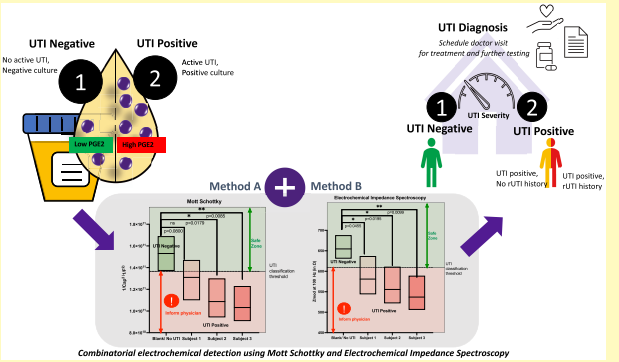

KEYWORDS: *Prostaglandin E2 (PGE2) biosensor, electrofluidic capacitor, recurrent urinary tract infection (rUTI), electrochemical impedance spectroscopy (EIS), Mott−Schottky (MS)*

With the current pandemic situation, one way of reducing the existing burden on the global healthcare system is by self-monitoring of diseases. This is especially valuable for diseases that demand regular intervention but are generally nonfatal when addressed in the early stages. One such condition, which affects around 150 million people worldwide and costs more than $1.6 billion annually, is urinary tract infection (UTI).[1] UTI is caused by the growth of pathogenic microorganisms (bacteria and sometimes fungi) in the urinary tract.[2] Since UTI does not fall under the category of mandatory infection to be reported in most countries, their detection and management are considered a lower priority by hospitals resulting in significant morbidity and mortality, especially in developing nations.[3] However, successful treatment of UTI is time sensitive, and if left untreated, UTI can ascend to the kidneys and spread to the bloodstream, and ultimately result in sepsis, renal damage, and even death.[4] Thus, early detection and regular monitoring of UTI symptoms is of paramount importance to ensure successful treatment.[5] UTI contributes to nearly 1% of ambulatory visits and around 7 million women visit the emergency department for UTI symptoms every year in the United States alone.[1] UTI is common in high-risk populations like infants, pregnant women, the elderly, patients with spinal injuries and/or catheters, and patients with immunocompromised conditions like diabetes mellitus and HIV infection.[5] The ability to reliably self-monitor UTI at home could be of great importance for demographic groups for whom unnecessary hospital exposure should be avoided.

Received: September 10, 2021
Accepted: December 6, 2021
Published: December 20, 2021

In many individuals, UTI will progress into a condition termed recurrent UTI (rUTI) defined as two or more episodes of UTI in 6 months or three or more episodes of symptomatic UTI in 12 months.[6] Recurrent UTI is associated with severe psychological and financial burden, especially among the elderly, and negatively impacts quality of life (QoL).[7] According to the European Center of Disease Prevention and Control (ECDC), the disease burden for UTI is as high as 81.2 disability-adjusted life years per 100 000 general population.[8] Recurrent UTI is also related to anxiety and depression in premenopausal women with reported depression rates as high as 61.9%.[9]

The current gold standard for UTI detection is clinical urine culture, which has a diagnostic period of 2−3 days.[5] During this diagnostic period, patients are often prescribed broad-spectrum antibiotics. However, this can lead to undesirable consequences like antibiotic resistance, alteration of the urinary tract microbiota, and increased medical costs.[10] Further, depending on the patient population, clinical urine culture can often suffer from diagnostic errors[11−15] because (i) the same microorganisms can cause UTI and asymptomatic bacteriuria (ASB)[16] and (ii) the urinary concentration of pathogenic microorganisms can often fall under the detection limit of standard clinical culture techniques.[4,17]

To overcome these limitations, several culture-independent alternatives have been developed. A comparison of these and other current UTI diagnostic methods and their limitations are presented in Table S1. Most of these methods are expensive, require sophisticated sample preparation and laboratory facilities,[18] and are limited by the breadth of the panel of pathogens detected[5,19] and, thus, are not ideal for routine screening, especially in home environments. For home-based point-of-care testing, a number of UTI diagnostic biosensors have been developed in the research space, which can be broadly categorized as (i) culture-based devices, (ii) (semi-)automated urine analyzers, and (iii) enzymatic assays.[5] The culture-based point-of-care tests (POCTs) suffer from turn-around times of 16−24 h for bacterial growth and quantification, which delays diagnosis.[5] The semiautomated urine analyzers and enzymatic assays are found in the form of urine dipsticks. Common urine dipsticks rely on the qualitative (colorimetric) detection of biomarkers like nitrites (waste of bacteria) or leukocyte esterase (white blood cells) and lack quantitation. Semiquantitative (colorimetric) or qualitative ("yes/no") readouts result in loss of concentration information and, hence, suffer from limited positive predictive capability.[5,20−22] Enzymatic assay-based UTI biosensors typically are label-based and require multistep sample preparation (fluorescent tagging) with amplification/enrichment to enhance target.[5]

A paradigm shift in UTI and rUTI management can be initiated by developing a simple and easy-to-use diagnostic device that can routinely monitor signs of UTI in the comfort of one's home. In this way, the device can provide an in-home test result that can be directly conveyed to the physician so they may initiate care and prescribe appropriate therapies. Key attributes of such a device would include (i) uncomplicated, single number readouts, (ii) cost effectiveness (especially for resource-challenged regions), (iii) high sensitivity and selectivity, (iv) rapid and early detection, (v) portability, and (vi) independence from the causative pathogen. In this regard, to truly achieve success for diagnosis along the lines of the most successful commercially available point-of-care diagnostic device, which is diabetes biosensor, it was important to look for a single, high sensitivity and selectivity biomarker of active UTI and rUTI. In their recent work, Ebrahimzadeh et al. showed that urinary Prostaglandin E2 (PGE2) is one such biomarker that can serve not only as a reliable diagnostic but also a prognostic biomarker for rUTI in postmenopausal women.[23] PGE2, which is an enzymatic product of cyclooxygenase-2 (COX-2), is a critical mediator of the inflammatory response.[24,25] Thus, PGE2 was chosen as the target biomarker to achieve early, accurate single number quantitative readouts, independent of the causative pathogen.[26] To produce a cost-effective, portable, rapid diagnostic device, electrochemical/electroanalytical methods were chosen as the transduction mechanism for biosensing. Electrochemical biosensors are popular for building POC devices as they are (i) small, portable, mass-producible, and inexpensive as they are compatible with microfabrication and (ii) are reliable as they seamlessly integrate with miniaturized electronics with high fidelity and are generally programmed to give out quantitative results.[27−29]

This study describes the development of a label-free, non-faradaic electrofluidic capacitor-based biosensor for PGE2 quantification in less than 60 μL of human urine. We demonstrate the use of PGE2, an attractive diagnostic and prognostic UTI biomarker, as an analyte for urine-based electrochemical biosensing. This novel work employs two powerful electroanalytical methods of electrochemical impedance spectroscopy and Mott−Schottky and is the first demonstration of using these two techniques to build an electrofluidic capacitor as a reliable and robust biosensor for PGE2. The sensor shows good sensitivity to PGE2 concentration (correlated with UTI severity) in both spike-in and patient urine samples for a wide urine pH range. Calibrated using both EIS and MS, the sensor is able to distinguish between UTI positive and negative urine samples. Spike and recovery studies show a high correlation between the measured and actual PGE_2 concentrations simulated for no, low, and high UTI severity. Attenuated total reflectance-Fourier transform infrared spectroscopy (ATR-FTIR) and surface plasmon resonance studies were performed to study the binding chemistry of assay stack elements. The surface charge and buffer effects were studied using dynamic light scattering experiments by measuring the ζ-potential and hydrodynamic radii of the unconjugated and conjugated capture probe under varied dosing (0, 500, 5000 pg/mL) and urine pH (5−8) conditions. Finally, observational human subject studies were done wherein patient urine samples were used to evaluate the efficacy of sensor performance and the impact of nonspecific constituents was studied.

EXPERIMENTAL SECTION

Materials and Reagents. Monoclonal α-PGE2 antibody was purchased from Arbor Assays (Ann Arbor, MI). The antibody was aliquoted and stored at 4 °C until further use. HPLC-purified PGE2 antigen was obtained in synthetic powder form from Sigma-Aldrich (St. Louis, MO). The crosslinker DSP (dithiobis (succinimidyl propionate)) and phosphate-buffered saline (PBS) were obtained from Thermo fisher Scientific Inc. (Waltham, MA). Artificial urine was prepared using the recipe (MP-AU or multipurpose-artificial urine) by Sarigul et al., and all of the dilutions were prepared in deionized water.[30] The urine buffer pH was adjusted using sodium hydroxide (10% NaOH) and hydrochloric acid (10% HCl) obtained from Sigma-Aldrich (St. Louis, MO). Pooled human urine samples (pH ~6.5) were obtained from Lee Biosolutions (St. Louis, MO).

https://doi.org/10.1021/acssensors.1c01951
ACS Sens. 2022, 7, 186−198

The sensor system was constructed using a Metrohm 220 AT three-electrode (gold working and counter electrode and silver reference electrode) screen printed sensor (Metrohm USA).

Immunoassay Design and Binding Chemistry Characterization. Figure 2 shows binding chemistry analysis of the immunoassay stack of the non-faradaic biosensor, which involves (i) binding between the DSP crosslinker and the monoclonal PGE2 antibody (mAb) and (ii) the subsequent capture and preferential binding of the PGE2 expressed in urine to the PGE2 mAb. Thus, the binding chemistry involved in the developed sensor stack was evaluated in two parts: first, attenuated total reflectance-Fourier transform infrared spectroscopy (ATR-FTIR) analysis was done to identify the optimal concentration of the monoclonal PGE2 antibody for sufficient chemisorption of the PGE2 antibody on the working electrode by studying the DSP−mAb binding chemistry. Second, surface plasmon resonance (SPR) analysis was done to validate the binding between the PGE2 mAb and the PGE2 molecule spiked in 1× PBS buffer.

Nicolet 6700 FTIR (Thermo Fisher Scientific) was used for the ATR-FTIR studies. A liquid sample of 10 mM DSP crosslinker dissolved in DMSO was used as the baseline for the analysis. A 1:1 mixture of PGE2 antibody in PBS and DSP crosslinker dissolved in DMSO was incubated for 2 h.[31] Various concentrations of PGE2 mAb, namely, 0.1 μg/mL, 1 μg/mL, 10 μg/mL, and 1 mg/mL conjugated to DSP were probed for thiol bond formation. For both the baseline DSP spectrum and the DSP−mAb conjugate spectra, 256 scans were collected, for a wavelength range of 4000−600 cm^{-1}, at a resolution of 4 cm^{-1}. To ensure sufficient sites for the subsequent capture of the target analyte, i.e., the PGE2 molecule expressed in urine, antibody saturation studies were performed (see Figure S2). From these experiments, the antibody loading capacity for the sensor (considering the area of the working electrode) was determined based on the variation in the modulus of impedance from the crosslinker functionalization step to the mAb immobilization step. After optimizing the PGE2 mAb concentration, the preferential binding of the PGE2 antigen to the PGE2 mAb due to affinity capture was studied using surface plasmon resonance experiments. SPR studies were performed using the Open SPR instrument (Nicoya, Canada) using PBS as the running buffer. Carboxyl sensor chips were used for binding characterization and NHS-EDC binding chemistry was used for validating the PGE2 antibody−antigen binding. All reagents, kits, and sensor chips were purchased from Nicoya (Canada). Two-channel mode was used, and the protocol provided with the carboxyl sensor kit tech guide was followed. The concentrations used for the reagents were 10 mM HCl (pH 2−3), 10 μg/mL PGE2 antibody, and 500 pg/mL (lowest concentration) PGE2 antigen.

ζ-Potential Studies. As shown in Figure 3A, the physiological urine pH range varies from 5 to 8 and the median human urine pH is 6.[32] Dynamic light scattering studies were done using Malvern Zetasizer NanoZS (Malvern Instruments, U.K.) to evaluate the surface charge and size variation of the developed PGE2 assay stack as a function of pH and dosing. Figure 3A shows the cases evaluated, namely, Blank (no PGE2), UTI negative (low PGE2), and UTI positive (high PGE2) cases.

The variation of the surface charge of the monoclonal PGE2 antibody was studied by measuring the ζ-potential for the entire physiologically relevant pH range of urine, that is, pH 5−8. Further, the effect on the overall surface charge of the antibody−antigen conjugate post binding was also visualized for the entire pH range of 5−8 for low, medium, and high concentrations of PGE2. ζ-Potential was calculated from the electrophoretic mobility of stack constituents using Smoluchowski's equation.[33] The size variation of the PGE2 mAb (measured as the hydrodynamic radius) due to the effect of bulk ions and buffer pH was studied. Further, the hydrodynamic radii of the PGE2 mAb and the PGE2 mAb conjugated to both low (UTI negative) and high (UTI positive) concentrations of PGE2 antigen expressed in artificial urine (pH 6) were measured.

Experimental Design for Dose-Response Curves for EIS and MS. The sensor consists of a standard three-electrode system made up of gold working and counter electrodes and silver reference electrodes screen printed on a ceramic substrate. Five microliters of 10 mM of a DSP crosslinker (dissolved in DMSO) was incubated only on the working electrode for 2 h in the dark for strong thiol bond formation. After DMSO wash and one 1× PBS wash, monoclonal PGE2 antibody was immobilized on the gold working electrodes in 5 μL of volume for overnight incubation for EDC-NHS bond formation. The crosslinker concentration was selected based on literature.[31,34] ATR-FTIR-based spectroscopic validation (described in previous sections) was used to validate the suitability of the selected incubation time and antibody concentration for urine prostaglandin E2 biosensing. The volume of 5 μL for the crosslinker and antibody was chosen to ensure that the entire working electrode (only WE) gets covered to ensure specificity of the response.

The physiological range for urine PGE2 is 500−5000 pg/mL.[23] Doses were prepared by spiking PGE2 antigen in synthetically prepared urine (pH 6) for urine PGE2 concentrations of 500, 1000, 2000, 3000, 4000, and 5000 pg/mL. The urine sample containing the antigen was incubated on the sensor surface for 5 min. This was done based on the findings from a recent study by Zorea et al., where it was found that for non-faradaic EIS, with increasing incubation times the measurable values of interfacial capacitance (constant phase element) and resistance (solution and diffusional resistance) decrease.[35] Calibration dose-response curves for EIS-based PGE2 detection in artificial urine (n = 3) and pooled human urine (n = 3) were reported as percentage changes in impedance modulus at 100 Hz relative to a baseline or zero dose as a function of PGE2 concentration. Calibration dose-response curves for MS-based PGE2 detection in artificial urine (n = 3) and pooled human urine (n = 3) were reported as percentage changes in $1/capacitance^2$ at 100 Hz relative to a baseline or zero dose as a function of PGE2 concentration.[36] Blank artificial urine buffer (pH 6) and unspiked pooled human urine were used as a baseline for developing calibration dose-response curves using artificial urine and pooled human urine, respectively. PGE2 ELISA (Enzo Life Sciences, Inc., Farmingdale, NY) was used to determine PGE2 levels in unspiked pooled human urine samples, which was found to be 639.17 pg/mL. The raw or absolute value data from pooled human urine (from which relative percent changes were calculated) for both EIS and MS have been included in Supporting Information (Figure S7). Since this value is below 2000 pg/mL, it was speculated that the PGE2 levels in the unspiked pooled human urine samples were representative of a healthy population cohort. Single-frequency EIS measurements (100 Hz) recorded impedance measurements over 5 min and were taken using a potentiostat (Gamry Instruments, Warminster, PA) after applying an AC excitation signal of 10 mV rms. MS measurements were carried out using the same potentiostat after applying a voltage from −0.5 to 0.5 V for 1 min. Extraction of the $1/capacitance^2$ for MS analysis was performed using Gamry Echem Analyst software. The choice of voltage inputs for the EIS and MS protocols was done such that an ohmic response is achieved without the denaturation of biomolecules.[37] Similar protocols were followed for the detection of PGE2 in pooled human urine. The data are represented as mean ± standard error of the mean (SEM).

Urine PGE2 levels are correlated with the risk of UTI onset and relapse. From literature, it has been found that urine PGE2 levels elevated above 2000 pg/mL are indicative of active rUTI in postmenopausal women and concentrations below this level are consistent with women who do not have active UTI or rUTI.[23] This threshold was utilized for spike and recovery analysis to evaluate the efficacy of dose-response experiments and the sensor's ability to distinguish between "no-UTI" and "active-UTI" cases (Figure 5). Thus, the signal response at PGE2 dose concentration of 2000 pg/mL was used as the threshold dose as the UTI classification threshold for classifying test urine sample as UTI positive or negative.

Urine pH Variation Study. The physiologically relevant pH range of human urine varies from 5 to 8. The effect of urine pH on the sensor's performance to detect PGE2 was studied. The artificial urine buffer was adjusted to 5, 6, 7, and 8 and was spiked with PGE2 antigen of concentration 500−5000 pg/mL. EIS and MS experiments were carried out as described in the previous section. Two other conventional DC-based electrochemical methods—chronoamperom-

https://doi.org/10.1021/acssensors.1c01951
ACS Sens. 2022, 7, 186−198

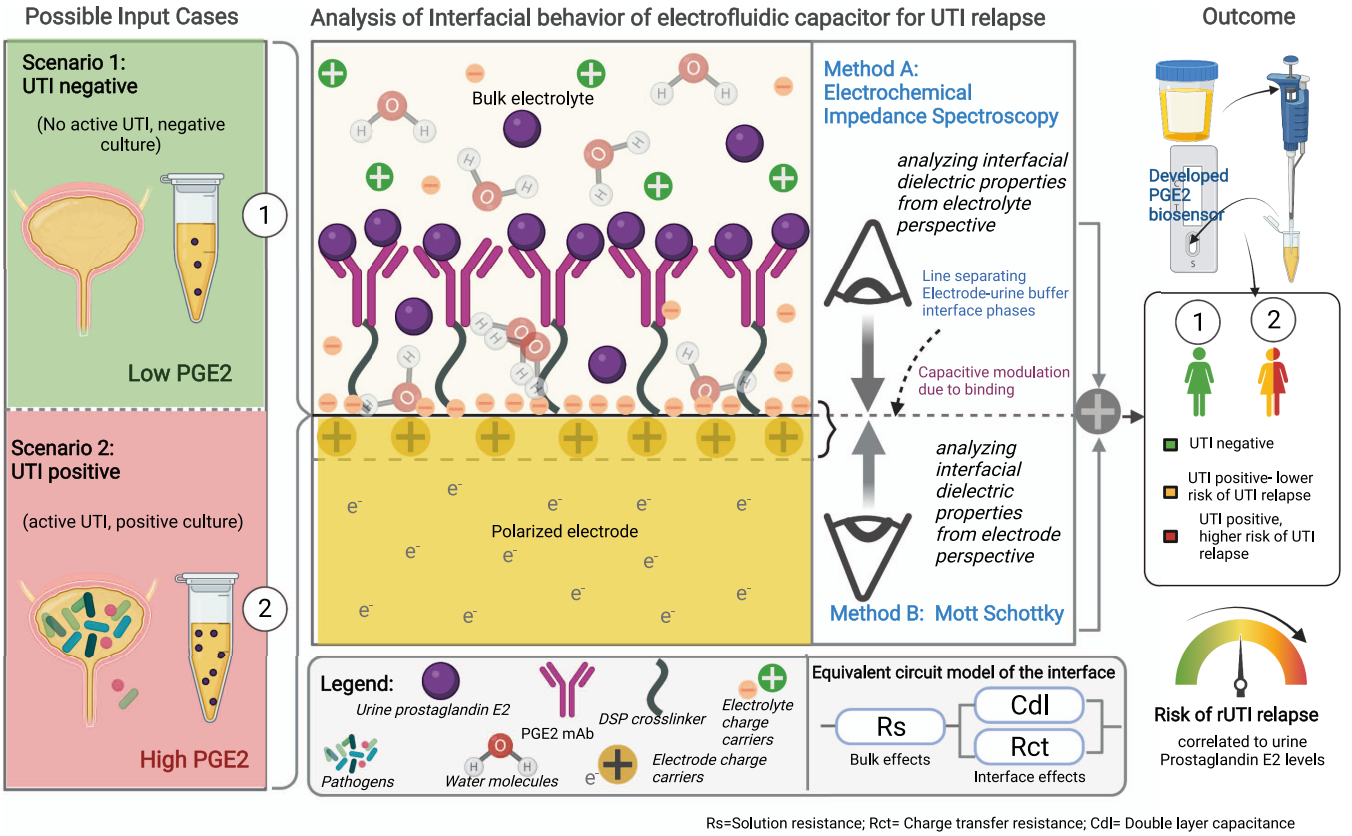

Figure 1. Schematic showing the construction and operation of the electrofluidic capacitor PGE2 biosensor. Created using Biorender.com.

etry (CA) and chronocoulometry (CC)—were studied (with similar inputs, i.e., −0.5 to 0.5 V for 1 min) to validate the suitability of the chosen techniques (i.e., EIS and MS) for building the electrofluidic capacitor. This has been discussed in further detail in the Results and Discussion section.

Spike-in and Recovery Studies. Figure 5 represents the results from the spike in and recovery analyses for both MS and EIS methods. In this experiment, known concentrations ("actual") of PGE2 spiked in triplicate were compared with the "measured concentration" calculated based on the previously developed calibration curves. Urine samples spiked with known PGE2 concentrations (spread over the dynamic range of the sensor) were analyzed using EIS and MS methods. The results obtained (i.e., modulus of impedance at 100 Hz for EIS and 1/capacitance^2 at 100 Hz for MS) were converted to "measured concentrations" by interpolation of X mean values calculated/recovered based on the curve fitting (sigmoidal, four parameter logistic regression, X is concentration; Least squares fit) based on the calibration dose studies for each method (Figure 4). Then, the correlation between the "actual" concentration (that is the known spiked concentration) and the "measured" concentration (obtained by interpolation from the fitted dose-response curve) was analyzed using R^2 values to study the accuracy of the measured values. The correlation between the spiked and recovery concentrations was analyzed using both methods (Figure 5A,B).

Human Subject Testing Studies. The human subject samples were collected as part of approved Institutional Review Board protocols (STU 082010-016, MR 17-120). Patient samples were collected during their visit at UTSW Medical Center and written consent was obtained prior to sample collection and participation in the study. As a proof of concept, three postmenopausal female subjects with active, symptomatic UTI as diagnosed by clinical urine culture were studied. Clean-catch urine collected from these patients was aliquoted and stored in −80 °C and was retrieved later for analysis. Urinary PGE2 and creatinine were measured via high sensitivity ELISA (Enzo) and Creatinine Urinary Detection Kit (Thermo Fisher Scientific) based on the instructions from the vendors. Urine was diluted 1:2 for PGE2 measurements and 1:20 for creatinine measurements. Optical density measurements for these colorimetric assays were performed with a Syngergy H1 plate reader (Biotek, Winooski, VT).[23] Figure 7C shows the setup for carrying out these experiments. Postanalysis was done using the calibration dose-response curves for both methods described in the previous sections. The signal response at PGE2 dose concentration of 2000 pg/mL of the control buffer, i.e., artificial urine (MP-AU) was used as the threshold dose as the UTI classification threshold for classifying test urine sample as UTI positive or negative.

Statistical Analysis. Data are represented as mean ± SEM. The data is represented with $n = 9$ ($n = 3$ intersensor and $n = 3$ intrasensor replicates). The significance test was carried out using Student's t-test and one-way ANOVA with α of 0.05. Nonlinear regression and other statistical analyses were performed using GraphPad Prism version 9.1.2 (GraphPad Software Inc., La Jolla, CA).

RESULTS AND DISCUSSION

Design of the Electrofluidic Capacitor-Based Biosensor. The sensor operates on the electrofluidic capacitance principle wherein the arrival of a fluid front (in this case urine buffer) changes the permittivity at the double layer interface.[38] This capacitive change is measured by planar metallic electrodes and correlated with the level of target analyte (in this case, PGE2). Electrofluidic capacitors have been widely used in the energy and fuel cell space; however, their use in biosensing is sparse.[39] This work discusses the development of a simple, planar electrofluidic capacitor that does not require any microfluidic channels for fluid storage for reliable sensing. A standard three-electrode electrochemical system serves as the base electrode of the electrofluidic capacitor, while the

https://doi.org/10.1021/acssensors.1c01951
ACS Sens. 2022, 7, 186−198

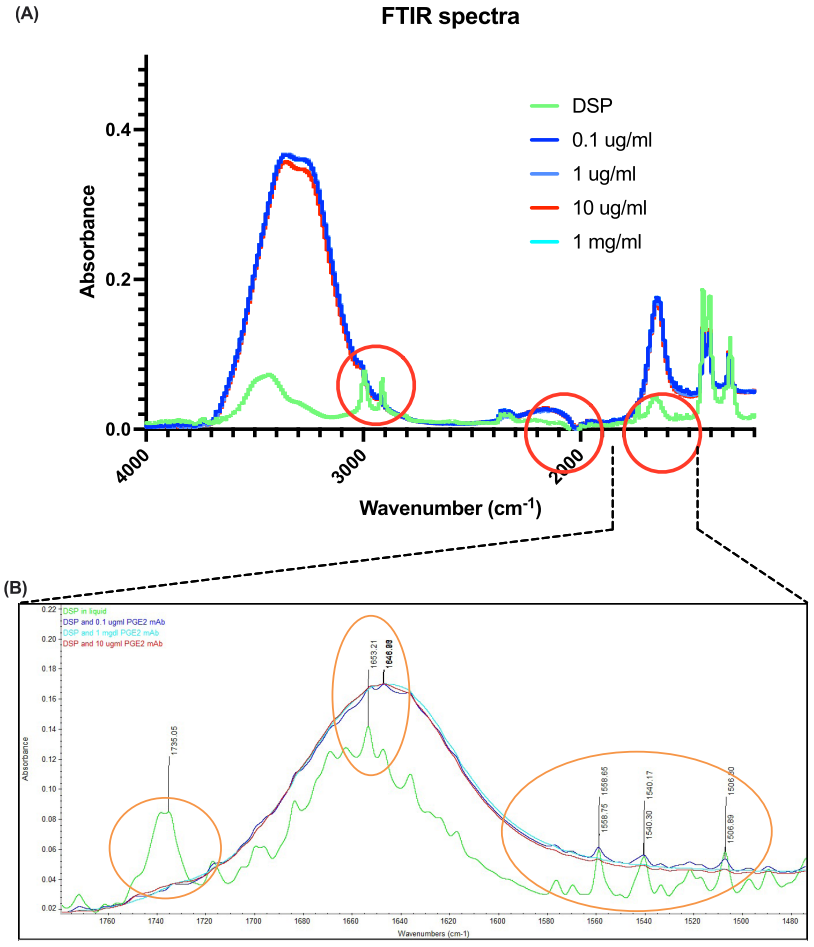

Figure 2. (A) ATR-FTIR spectra of a DSP crosslinker and PGE2 antibody conjugated to DSP and (B) inset showing the measured peaks characterizing the binding chemistry between the crosslinker and antibody.

urine buffer acts as the dielectric medium. The choice of electrochemical methods for building the capacitor was based on down selecting techniques that are capable of tracking subtle changes due to binding without being affected by ionic noise due to urine buffer pH variation. Two DC-based techniques, namely, chronoamperometry (CA) and chronocoulometry (CC) and two AC-based techniques, namely, electrochemical impedance spectroscopy (EIS) and Mott−Schottky (MS) were employed for the studies keeping the input parameters similar (as listed in the Experimental Section). Figure S3 shows the response from CA and CC as a function of PGE2 dosing for a pH range of 5−8. Clearly, the response from the methods CA and CC are largely affected by the urine buffer pH and give a stable response for 7 or above. Since the normal urine pH is slightly acidic and the median value is 6, EIS and MS were selected for the calibration of the electrofluidic capacitor-based PGE2 biosensor, which exhibits superior and consistent dose-dependent response independent of urine pH levels. This is because unlike CA and CC, which capture the bulk effects of the electrolyte, EIS and MS focus on subtle changes at the electrical double layer interface.[37,40−42]

To study the capacitive properties of the electrical double layer (EDL) developed at the electrode−urine buffer interface as a result of analyte-capture probe binding, electrochemical impedance spectroscopy (EIS) and Mott−Schottky (MS) were used. Both methods are highly established and widely used for capacitive analysis (equivalent electrical circuit shown in Figure 1), especially in the field of biosensing as they are AC based, compatible with small-signal analysis, and suitable when working with proteins to avoid denaturation and compromise of structural integrity.[37] While EIS provides a powerful means of analyzing subtle biosensing events from the electrolyte (i.e., urine buffer) side, MS allows for robust evaluation of modulation of dielectric interfacial properties from the electrode side.[36,41] By combining these two complementary and powerful techniques, a holistic and accurate analysis of electrochemical phenomena can be achieved (see Figure 1). The use of urine as the diagnostic biofluid media affords several advantages. Urine, being highly ionic, serves as a high conductivity medium suitable for developing capacitive systems.[43] This means that the electrical signal, in its original, unamplified form, can be detected without significant electrode modification or the additional step of labeling or redox tagging. Further, urine has sufficient residence time in the bladder for the diffusion of proteins, metabolites, salts, etc., from surrounding blood vessels, which makes it a reliable diagnostic biofluid, especially for analytes associated with early disease detection which are expressed in low concentrations initially.[44] Another added advantage of urine is that this diffusion process results in a low concentration of interferents and other biomolecules which are nonspecific to the sensor, which allows for low inherent noise for the capacitive system. In this way, the utilization of EIS and MS in the form of a label-free electrofluidic capacitor-like biosensor to detect PGE2 levels in

https://doi.org/10.1021/acssensors.1c01951
ACS Sens. 2022, 7, 186−198

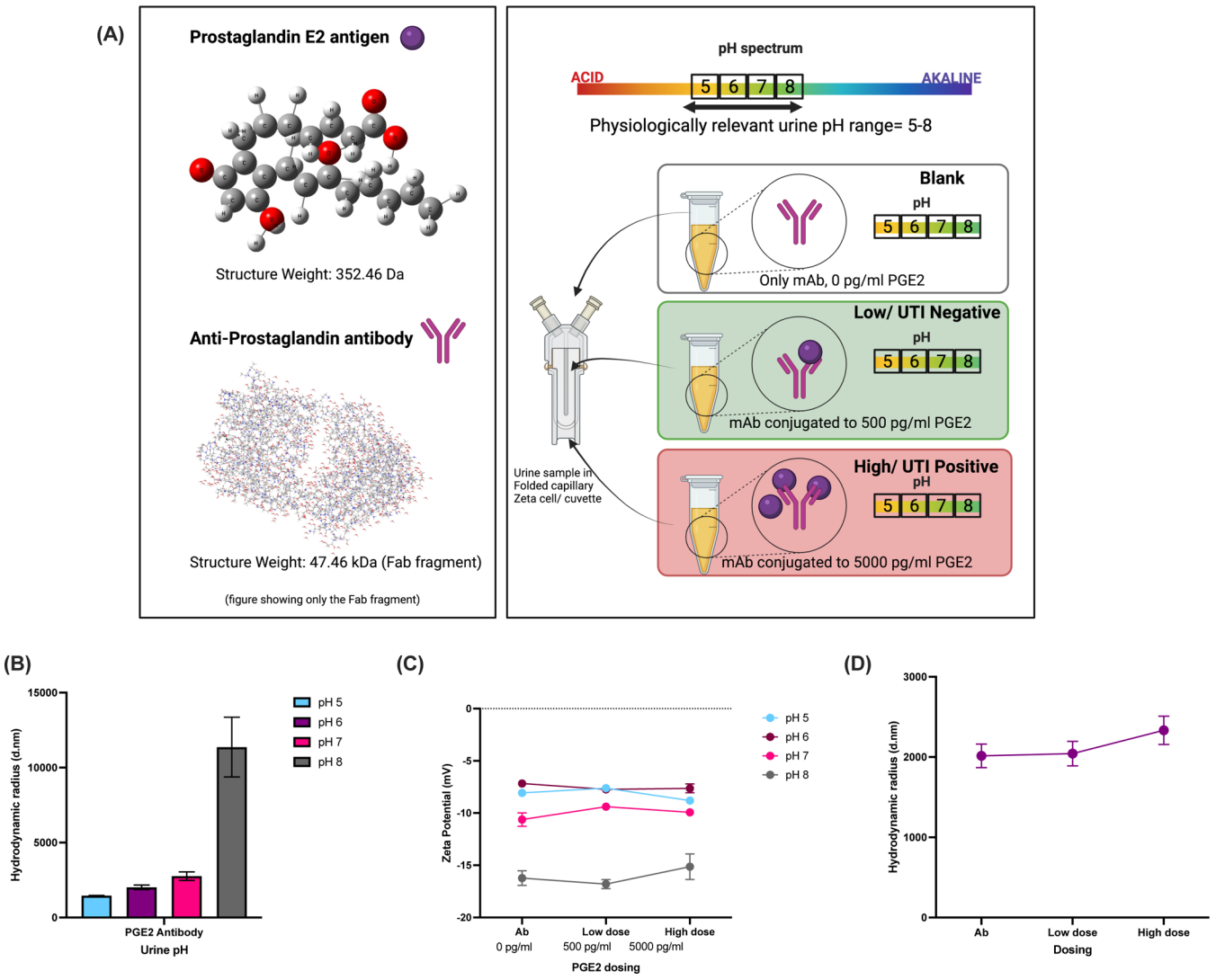

Figure 3. ζ-Potential studies: (A) schematic showing the mass comparison of the capture probe (PGE2 antibody) and target analyte (PGE2 antigen), physiologically relevant urine pH range, and dynamic light scattering experiments conducted for evaluating binding between the PGE2 antibody and 0, 500, and 5000 pg/mL PGE2—corresponding to blank, UTI negative, and UTI positive—at pH 5–8, (B) hydrodynamic radius variation of PGE2 antibody in urine for pH 5–8, (C) ζ-potential variation of sensor stack elements as a function of pH (5–8) and dosing (0, 500, and 5000 pg/mL), and (D) hydrodynamic radius variation of antibody–antigen complex as a function of PGE2 antigen dosing for urine pH 6 (median human urine pH). Partially created using Biorender.com.

neat (unprocessed/unfiltered) human urine can be a simple yet effective self-monitoring solution for reliable and rapid home-based UTI management.

Validation of Binding Chemistry. The proposed PGE2 sensing scheme involves the affinity-based capture of PGE2 molecules expressed in urine using a highly specific monoclonal PGE2 antibody. The antibody is bound to the working electrode via strong thiol bonds using a DSP crosslinker. The formation of a self-assembled monolayer of the mAb on the working electrode region is validated using ATR-FTIR analysis. When PGE2 is present in urine, it preferentially binds to the monoclonal antibody by affinity capture. The peaks specific to the DSP crosslinker and the binding between the DSP and PGE2 mAb have been identified. Figure 2B shows the zoomed-in spectra for the DSP baseline and the DSP–mAb conjugates. Due to its primary amine structure, the antibody binds to the DSP crosslinker by cleaving the N-hydroxysuccinimide (NHS)–ester bond. This breakage of CO–NHS bond of DSP due to NHS binding of DSP linker to PGE2 mAb was validated by the decrease of a peak at 1735.05 cm^{-1}. Further, a shift in primary amide peak from 1653.21 to 1646.98 cm^{-1} as a result of binding and formation of stable secondary amide peaks at 1500–1550 cm^{-1} was observed. Similar peaks were observed for all of the test concentrations of PGE2 mAb. In this way, the binding chemistry between the crosslinker and PGE2 mAb was validated. The stock PGE2 mAb solution (100 μg/mL) purchased from the vendor had 0.09% sodium azide present in it to prevent microbial contamination. Through the ATR-FTIR experiments, it was also confirmed that sodium azide does not impact binding (even for the lowest tested mAb concentration, i.e., 0.1 μg/mL) and its removal is not required (as evident from the position of actual peaks).

Next, antibody saturation studies were performed to identify the antibody loading capacity at the working electrode of the sensor (Figure S2). It was found that for the given working electrode area and its optimized sample volume (i.e., 5 μL), the signal response saturates after 5 μg/mL, meaning that

https://doi.org/10.1021/acssensors.1c01951
ACS Sens. 2022, 7, 186–198

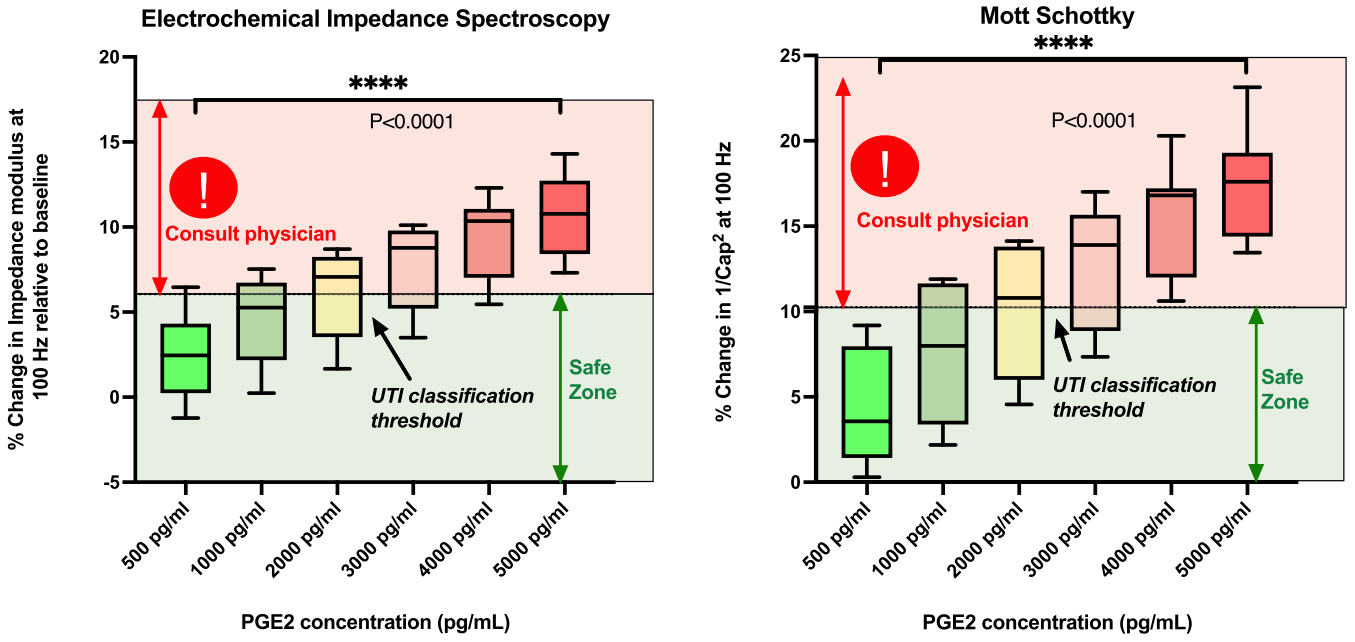

Figure 4. Calibration dose-response in pooled human urine for low, medium, and elevated PGE2 levels for EIS and MS.

antibodies bind to the DSP crosslinker self-assembled monolayer and provide sufficient binding sites for PGE2 analyte molecules in urine. Based on these results and by considering the urine sample volume (i.e., 60 μL sufficient to cover all three electrodes to complete the electrical circuit) and the desired sensor dynamic range (i.e., 500−5000 pg/mL of PGE2), 10 ug/mL was chosen as the optimal PGE2 mAb concentration optimized for further biosensing.

To validate the reliable affinity capture of PGE2 analyte molecules by the PGE2 mAb at the optimized concentration, SPR studies were performed for the lowest PGE2 concentration, i.e., 500 pg/mL. Figure S4 shows the signal response for various steps of the protocol. As per the protocol outlined by the vendor, Channel 1 corresponds to the nonspecific binding (only the PGE2 antigen in the running buffer is flowed through this channel) activities, while channel 2 corresponds to the specific binding events between the PGE2 mAb and Ag (both Ab and Ag flow through this channel). From the inset, by comparing the response from both the channels, it is clear that PGE2 is successfully immobilized onto the gold carboxyl sensor chips and the binding between optimized PGE2 mAb and the lowest dose of PGE2 antigen is also validated for subsequent electrochemical biosensing.

Effect of Surface Charge on Binding. The proposed biosensor is label free and operates in non-faradaic mode since there is no exchange of charges between the electrode and the electrolyte. The binding between the antibody and antigen modulates the interfacial dielectric constant due to the accumulation of analyte molecules and the rearrangement of water and ions at the EDL. To study the electrochemical and physical properties of different elements of the assay stack, dynamic light scattering experiments were done to measure the surface charge (using ζ-potential) and the size (using hydrodynamic radius). ζ-Potential is the potential measured at the plane that separates the stern and diffuse layers of the EDL.[45,46] To get an overall picture of the interfacial charge, the entire physiological range of urine pH was studied (i.e., pH 5−8). Smoluchowski's equation for electrophoretic mobility was utilized. The size of the antibody and the antibody−antigen complex at pH 5−8 were probed measuring the hydrodynamic radii, which is calculated based on the Brownian motion and the diffusion coefficient of the molecules suspended in the artificial urine buffer.[47]

Figure 3A shows the structure of PGE2 antigen and the molecular weight comparison of the PGE2 antibody and antigen. As shown in the figure, for ζ-potential and hydrodynamic radius studies, the urine pH was varied between 5 and 8, and the concentration of the PGE2 antigen was 0 (blank, only mAb), 500 (low concentration, no UTI), and 5000 pg/mL (high concentration, active UTI).

The assay consists of the monoclonal PGE2 antibody covalently bound to the thiol linker by NHS ester linkage. Next, PGE2 Ag expressed in urine preferentially binds to PGE2 mAb by affinity capture. From Figure 3B, the hydrodynamic radius of the antibody increases with pH as more and more hydroxyl ions in the buffer populate the stern and diffuse layers. Next, as can be seen in Figure 3D, with dosing, the size of the antibody−antigen conjugate increases as more and more PGE2 antigen present in the buffer binds to the antibody. As shown in Figure 3C, the ζ-potential of the antibody−crosslinker conjugate and Ab−Ag conjugate were found to be negative at urine pH 5−8. A high negative ζ-potential indicates that the complex is stable and not prone to agglomeration. As the amount of hydroxyl ions increases with pH, the surface charge becomes increasingly negative, as evidenced by the increase in negative ζ-potential. Figure 3C also shows that as we go from low to high PGE2 doses, the ζ-potential effectively remains unchanged for a given pH. This validates that PGE2 is an uncharged or minimally charged molecule and the capacitive response signal response is achieved due to antigen−antigen binding and not due to crosstalk from electrostatic noise from the bulk solution. In this way, high signal-to-noise ratio was achieved, by suppressing the effect of electrostatic noise (from the highly ionic urine buffer) and charge screening effects, which is especially important in a non-faradaic setting where no redox labels are used for signal enhancement.

https://doi.org/10.1021/acssensors.1c01951
ACS Sens. 2022, 7, 186−198

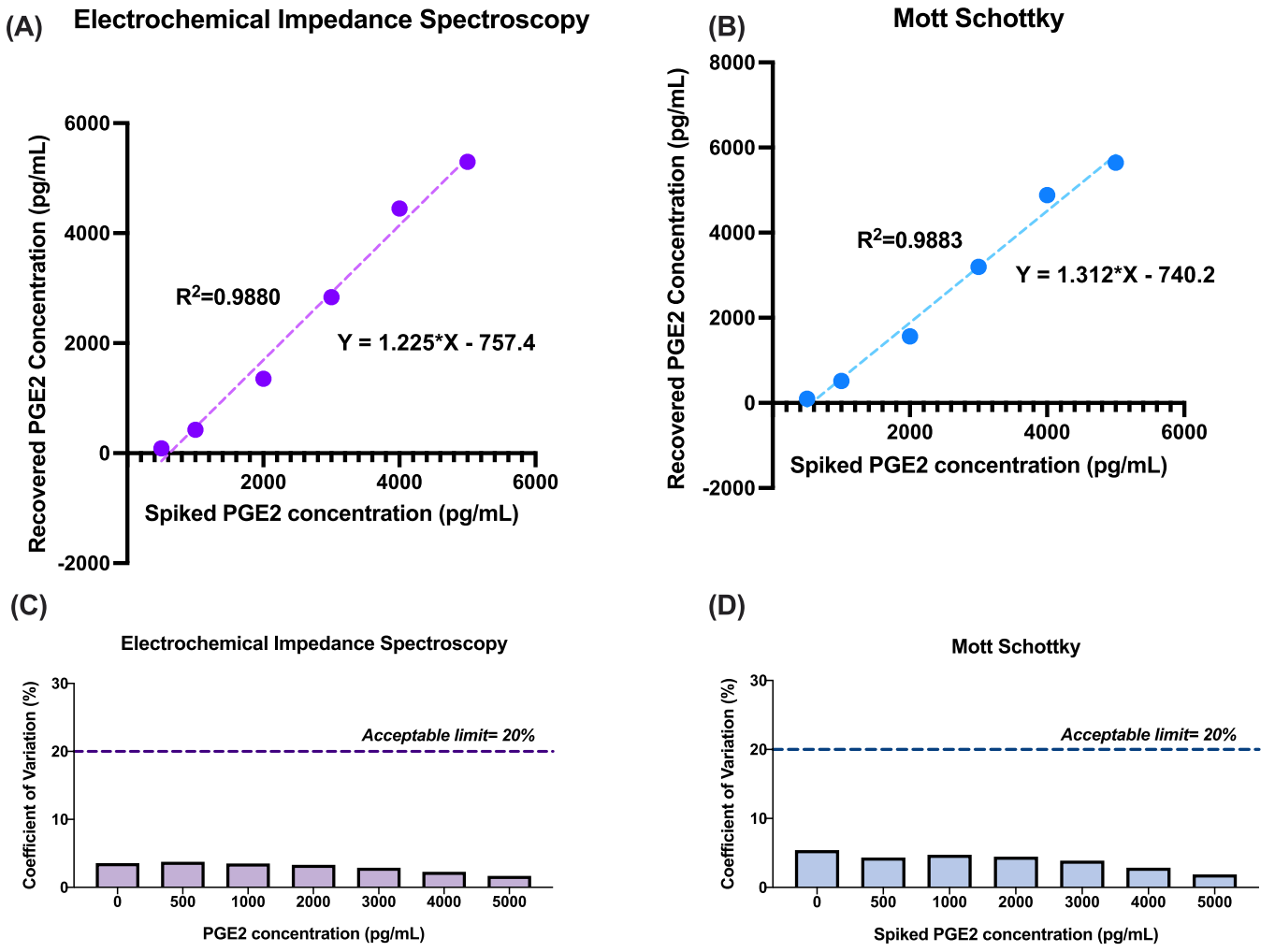

Figure 5. Spike and recovery experiments for (A) EIS and (B) MS showing a correlation between actual concentration (i.e., the known spiked concentration) versus measured concentration (i.e., the PGE2 concentration recovered using interpolation of the fitted dose-response curve) in urine. Coefficient of variation (CV%) analysis for (C) EIS and (D) MS methods.

Calibration of the Sensor in Pooled Human Urine. Modulation of dielectric properties at the electrode−urine buffer interface and a rearrangement of ions and water molecules, due to Ab−Ag binding, were captured using two powerful AC-based electroanalytical techniques, namely, electrochemical impedance spectroscopy (EIS) and Mott−Schottky (MS). In these techniques, a small sinusoidal AC voltage is applied at the working electrode, and a phase-shifted current is obtained as the output. In EIS, the ratio of the input voltage to the output current gives a complex impedance characteristic of the biosensing system (correlated with the binding activity at a given analyte concentration).[37,40,48−50] The schematic in Figure S1 depicts the inputs and the corresponding outputs for different PGE2 levels in the test urine sample. In EIS, the modulus of the impedance is reported at a particular frequency and in MS, 1/capacitance^2 value is extracted. Both these parameters contain information regarding the capacitive makeup of the interface, which has been combinatorially leveraged to calibrate the sensor to obtain dose-response curves. The physiologically relevant PGE2 level in human urine ranges from 500 to 5000 pg/mL.[23] Figure S9 shows the characteristic response curves for both EIS and MS methods. Calibrated sensor dose responses for PGE2 detection in synthetic urine (pH 6) are depicted in Figure S5. Figure 4 shows the dose-response curve for PGE2 detection in pooled human urine. A linear dose response for synthetic urine (n = 3) and pooled human urine (n = 3), for a wide dynamic range of 500−5000 pg/mL, was observed for both methods, as shown in Figures 4 and 5. The modulus of impedance decreases in a dose-dependent fashion as the system becomes increasingly capacitive due to binding. Data are represented as mean ± SEM. The data is represented with n = 3 intersensor and n = 3 intrasensor replicates. The significance test was carried out using one-way ANOVA with α of 0.05. One-way ANOVA analysis results confirm that the sensor is capable of distinguishing between low, medium, and high levels of PGE2 in both artificial (pH 6) and pooled human urine (p-value < 0.0001). In this way, the electrofluidic capacitor-based biosensor was calibrated for urine PGE2 quantification.

Spike-in and Recovery and Precision Analysis. The accuracy of the biosensor performance for both EIS and MS was tested by spike-in and recovery studies. In this experiment, known concentrations (actual) of PGE2 spiked in triplicate were compared with the measured concentration calculated based on the previously developed calibration curves. Figure 5 shows the results of spike-in and recovery experiments done using PGE2 spiked in synthetic urine (500−5000 pg/mL). For both methods, a good correlation between the actual (spiked)

https://doi.org/10.1021/acssensors.1c01951
ACS Sens. 2022, 7, 186−198

concentration measured and the concentration (interpolated using the 4PL method) with R^2 value >0.98 was achieved. Thus, it was concluded that the developed sensor can reliably detect PGE2 levels present in neat urine with high accuracy. In this way, by probing the electric double layer from both the electrode (MS) and electrolyte (EIS) sides by leveraging the complementary robustness of both methods, a high sensitivity (1.312 for MS and 1.225 for EIS) was achieved by discarding the bulk effect of ions and minimizing the impact of the complex neat urine matrix in a label-free, simplistic, non-faradaic manner.

To evaluate the precision of both the EIS and MS techniques, the coefficient of variation (CV%) was calculated by averaging over all of the replicates as a function of the PGE2 levels spiked in urine samples. It was found that the CV% all of the PGE2 doses fall well within the acceptable range of 20% set by Clinical Laboratory Standards Institute (CLSI) guidelines.[51,52] In this way, it was concluded that the sensor is capable of precise measurements urine samples using both EIS and MS methods.

Effect of Cross-Reactive Molecules and Urine pH on Electrochemical Sensor Performance. To evaluate the selectivity and specificity of the developed sensor, cross-reactivity experiments were performed. To test if the sensor gives nonspecific signals for structurally similar prostaglandins in urine, the sensor was tested with Prostaglandin D2 for specificity and selectivity. PGE2-specific mAb was immobilized on the sensor, which was challenged with the threshold concentration, i.e., 2000 pg/mL of PGD2. Similarly, cross-reactivity studies were done to study the impact of urea (major constituent of urine ∼1.5 g/100 mL) on sensor performance. Figure 6 shows the results of cross-reactivity experiments. The data is represented with n = 9 (n = 3 intersensor and n = 3 intrasensor replicates) for PGD2 (2000 pg/mL) and urea (2000 pg/mL). The significance test was carried out using one-way ANOVA with α of 0.05. Clearly, the signal response for the interferent molecules lies well below that for the target PGE2 molecules at the UTI threshold concentration. One-way ANOVA shows a $p < 0.05$ for both EIS and MS, meaning that there is a significant difference in the sensor response for the same concentration of the specific (i.e., PGE2) and nonspecific urine constituents (i.e., PGD2 and urea). Thus, from these experiments, it is evident that the system is specific and selective for the target biomarker. The signal for PGE2 does not cross-react with that due to interferent molecules, and the sensor is able to significantly discriminate between UTI positive and UTI negative cases. The signal response at PGE2 dose concentration of 2000 pg/mL of the control buffer, i.e., artificial urine (MP-AU) was used as the UTI classification threshold. The effect of urine creatinine levels on the sensor response has also been studied and has been discussed in the Human Subject Testing Studies section.

Figure S6 shows the results of the evaluation of the effect of urine pH on the performance of the electrofluidic urine biosensor. The pH of urine was varied between 5 and 8 and the response of the sensor was studied using both EIS (Figure S6A−D) and MS (Figure S6E−H). For MS, using one-way ANOVA analysis, it was found that the sensor was able to reliably discriminate between the blank, low, medium, and high PGE2 levels (i.e., p-value < 0.05) for pH 5−8. For EIS, using one-way ANOVA analysis, it was found that the sensor was able to reliably discriminate between the blank, low, medium, and high PGE2 levels (i.e., p-value < 0.05) for pH 5−7. For pH

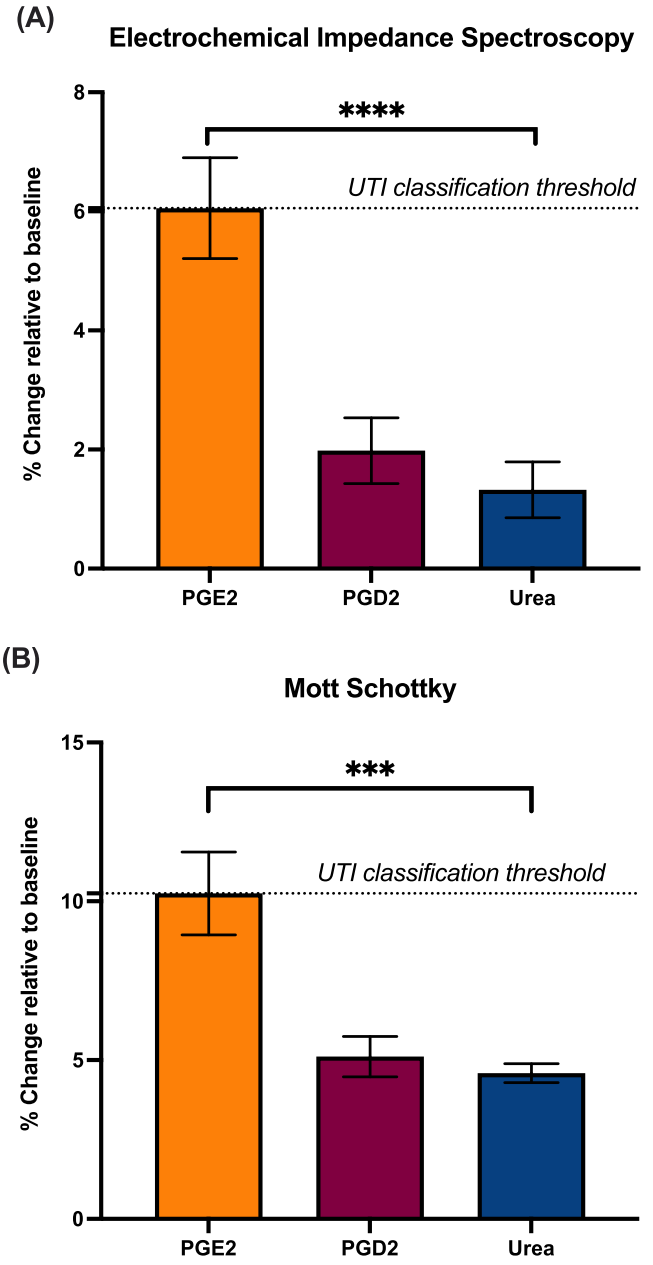

Figure 6. Cross-reactivity experiments with PGD2 and urea using (A) EIS and (B) MS. UTI classification threshold corresponds to the specific response of the PGE2 sensor for the threshold dose (i.e., 2000 pg/mL) for classifying UTI positive and UTI negative cases.

8 (abnormally high pH), a nonsignificant difference was obtained for EIS. Figure S3 shows the response from chronoamperometry (CA) and chronocoulometry (CC) as a function of PGE2 dosing for a pH range of 5−8. From this figure, it is evident that the two established DC-based methods of CA and CC fail to give an intelligible sensor response at low urine pHs but give a measurable dose-dependent response at neutral and pH. This is probably because at low pH levels the levels of small and mobile H+ ions are high, which contributes to considerable bulk noise. Since the DC-based CA and CC methods focus on overall bulks, they are not immune to this noise. However, this is not observed in the case of AC-based methods, EIS and MS, because in these methods, the modulation at the electrical double layer interface is predominantly studied (R_{ct} and C_{dl}). This validates the choice

https://doi.org/10.1021/acssensors.1c01951
ACS Sens. 2022, 7, 186−198

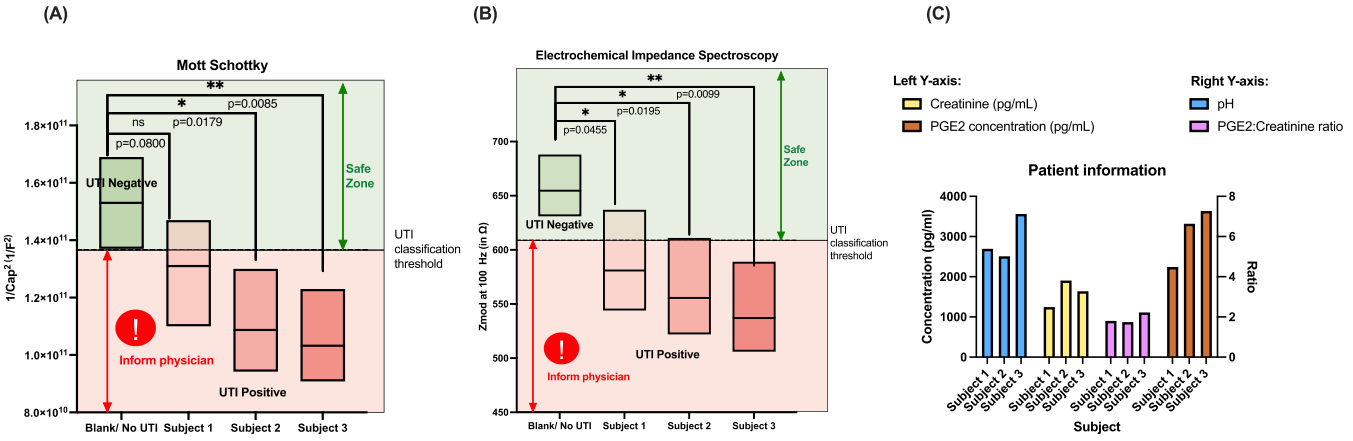

Figure 7. Result of human subject studies for (A) Mott−Schottky and (B) electrochemical impedance spectroscopy. (C) Mean values of creatinine and PGE2 levels obtained from ELISA analysis and pH and PGE2/creatinine ratio for the human subjects studied.

of using AC-based methods of EIS and MS when dealing with unfiltered or neat urine samples in label-free or non-faradaic formats.

Evaluation of Sensor Performance for Human Subject Testing. The proposed application and scope of the developed sensor are depicted in Figure 7. To test the efficacy of the proposed biosensing scheme on patient urine samples, non-faradaic EIS and MS measurements were run on urine samples obtained from three female human subjects. All patients fell under the category of postmenopausal women with active UTI. The blank/no UTI samples were from commercially obtained pooled urine collected from normal human donors (>3 donors per pool), which was considered as the baseline. The impedance values obtained were averaged (n = 3 sensors) and the trend was analyzed. As seen in Figure 7A,B, UTI threshold classification was done based on the mean values obtained during calibration using spiked urine samples. It was observed that the sensor could differentiate between healthy and unhealthy cases based on the signal output resulting from the PGE2 levels in the samples. This means that the subjects for whom PGE2 levels were beyond the threshold (denoted by the red area labeled "inform physician") need to inform their physician and discuss further testing and treatment options. Since the prescription of antibiotics is time-critical, this sensing approach will enable clinicians to ensure higher rates of treatment success. Using one-way ANOVA, it was found that the sensor is able to reliably discriminate between no UTI and possible UTI cases (one-way ANOVA, $p < 0.05$). As shown in Figure 7A,B, the data obtained from all three subjects was also evaluated using unpaired t-tests (one-sided, $\alpha = 0.05$). Figure 7B shows that the sensor was able to distinguish each of the unhealthy subject samples from the healthy/low PGE2 sample. Using the MS method (Figure 7A), the sensor was capable of showing a significant difference between only two unhealthy subject samples from the healthy/low PGE2 sample. However, since the electrofluidic capacitor biosensor relies on the outputs from both MS and EIS, overall, the sensor can discriminate between UTI positive (above 2000 pg/mL) and UTI negative cases (below 2000 pg/mL) reliably. This also emphasizes that a combinatorial approach employing both MS and EIS is necessary for preliminary diagnosis. Figure 7C shows the mean PGE2 and creatinine concentrations present in the human subject samples obtained using ELISA analysis and the corresponding PGE2: creatinine ratios and pH values of the patient urine samples. By comparing the PGE2 values (shown in orange in Figure 7C) and the sensor response in Figure 7A using both EIS and MS methods, it was clear that the sensor output was able to follow the trend of PGE2 concentration (was able to discriminate between the low to high levels) and was unaffected by the levels of creatine and pH value of each patient sample (Figure 7C). In this way, it was concluded that the sensor is capable of accurately identifying the presence of urinary tract infection in a rapid, label-free, and non-culture-based manner.

CONCLUSIONS

This work describes the development of an electrochemical, non-faradaic immunosensor for the quantification of prostaglandin E2 in neat human urine, in microliter volumes. To our knowledge, in this work, we have demonstrated the first label-free, non-faradaic electrofluidic capacitance-based PGE2 for measuring the levels of inflammation due to underlying infection. The binding chemistry involved in the various steps of the sensor stack was evaluated using spectroscopic techniques of ATR-FTIR and SPR. The electrochemical behavior of the sensor and the surface charge of its elements were studied using ζ-potential measurements. Non-faradaic single-frequency electrochemical impedance spectroscopy and Mott−Schottky analysis was used to study the capacitive modulation of the electric double layer as a function of the binding. Linear calibration dose-response curves were obtained for PGE2 dynamic range of 500−5000 pg/mL. Spike-in and recovery experiments were done to test the efficacy of the developed dose-response curves and were found to satisfy the analytical chemistry standards. The sensor did not show susceptibility to noise due to cross-reactive interferents and nonspecific buffer constituents in human subject samples. Finally, the performance of the device was assessed using patient urine samples. It was found that the sensor is capable of discriminating between low and high PGE2 levels and was able to identify the presence of UTI in three postmenopausal women. It was concluded that the sensor is capable of reliably discriminating between high (UTI) and low (no UTI) PGE2 concentrations for the entire physiologically urine pH range. A high signal-to-noise ratio and significant sensitivity for PGE2 detection for a wide dynamic range of 500−5000 pg/mL in neat/unfiltered urine was achieved by achieving high capacitive

https://doi.org/10.1021/acssensors.1c01951
ACS Sens. 2022, 7, 186−198

signal by holistically probing the electrical double layer interface from both the electrode and electrolyte aspects and by getting rid of the impact of the high noisy and ionic urine buffer matrix. The proposed biosensor has the potential for use a home-based UTI screening tool that will help patients for early detection of UTI. This will also assist clinicians in timely and precise antibiotic stewardship toward UTI management. Future research directions include translation of the electrofluidic sensing scheme into a portable form factor by interfacing with a miniaturized electroanalysis platform. In this way, the proposed novel electrofluidic capacitor-based biosensing scheme shows promise for being extended to incorporate other UTI-relevant biomarkers toward rapid, easy, and accurate home-based multiplexed testing in real-life practice.

■ ASSOCIATED CONTENT

Supporting Information

The Supporting Information is available free of charge at https://pubs.acs.org/doi/10.1021/acssensors.1c01951.

Table listing current methods of UTI detection, schematic representing inputs and outputs of the proposed sensor, figure showing results of antibody saturation studies, figure showing results from DC techniques, figure showing results from surface plasmon resonance studies, figure showing the calibration dose-response data obtained from spiked artificial urine samples, figure showing the evaluation of effect of the urine pH on sensor performance, figure showing the raw values of calibration dose-response data obtained from spiked pooled human urine samples, and figure showing the effect of the buffer matrix on the detection limit of the sensor, characteristic response plots for MS and EIS experiments (PDF)

■ AUTHOR INFORMATION

Corresponding Author

Shalini Prasad − *Department of Bioengineering, University of Texas at Dallas, Richardson, Texas 75080, United States;* orcid.org/0000-0002-2404-3801; Email: Shalini.Prasad@utdallas.edu

Authors

Antra Ganguly − *Department of Bioengineering, University of Texas at Dallas, Richardson, Texas 75080, United States*

Tahmineh Ebrahimzadeh − *Department of Biological Sciences, University of Texas at Dallas, Richardson, Texas 75080, United States*

Philippe Zimmern − *Department of Urology, University of Texas Southwestern Medical Center, Dallas, Texas 75390, United States*

Nicole J. De Nisco − *Department of Biological Sciences, University of Texas at Dallas, Richardson, Texas 75080, United States;* orcid.org/0000-0002-7670-5301

Complete contact information is available at: https://pubs.acs.org/10.1021/acssensors.1c01951

Author Contributions

S.P., A.G., N.J.D.N., and P.Z. conceived the project framework and designed the experiments. S.P. and A.G. designed the experiments, and A.G. performed the experiments. T.E. obtained the data for ELISA validation experiments. A.G. and S.P. wrote the article. N.J.D.N., P.Z., and T.E. reviewed the manuscript. S.P. and N.J.D.N. obtained funding. All authors have given approval to the final version of the manuscript.

Funding

This work was funded in part by the Welch Foundation (Grant AT-2030-20200401 to N.J.D.N.).

Notes

The authors declare the following competing financial interest(s): S.P. has a significant interest in EnLiSense LLC, a company that may have commercial interest in the results of this research and technology. The potential individual conflict of interest has been reviewed and managed by the University of Texas at Dallas, and it played no role in the study design; the collection, analysis, and interpretation of data; the writing of the article; or the decision to submit the article for publication.

■ ABBREVIATIONS

PGE2, Prostaglandin E2; rUTI, recurrent urinary tract infection; EIS, electrochemical impedance spectroscopy; MS, Mott−Schottky; ATR-FTIR, attenuated total reflectance-Fourier transform infrared spectroscopy; SNR, signal-to-noise ratio; SST, specific signal threshold; EDL, electrical double layer; ELISA, enzyme-linked immunosorbent assay

■ REFERENCES

(1) Öztürk, R.; Murt, A. Epidemiology of Urological Infections: A Global Burden. *World J. Urol.* **2020**, *38*, 2669−2679.

(2) Flores-Mireles, A. L.; Walker, J. N.; Caparon, M.; Hultgren, S. J. Urinary Tract Infections: Epidemiology, Mechanisms of Infection and Treatment Options. *Nat. Rev. Microbiol.* **2015**, *13*, 269−284.

(3) Foxman, B. The Epidemiology of Urinary Tract Infection. *Nat. Rev. Urol.* **2010**, *7*, 653−660.

(4) Grabe, M.; Bartoletti, R.; Bjerklund-Johansen, T. E.; Cai, T.; Çek, M.; Koves, B.; Naber, K. G.; Pickard, R. S.; Tenke, P.; Wagenlehner, F.; Wullt, B. *Guidelines on Urological Infections*; European Association of Urology, 2015.

(5) Murgia, L.; Stalio, O.; Arienzo, A.; Ferrante, V.; Cellitti, V.; Somma, S.; Di Visca, P.; Antonini, G. Management of Urinary Tract Infections: Problems and Possible Solutions. In *Urinary Tract Infection − The Result of the Strength of the Pathogen, or the Weakness of the Host*; InTech, 2018.

(6) Malik, R. D.; Wu, Y.; Christie, A. L.; Alhalabi, F.; Zimmern, P. E. Impact of Allergy and Resistance on Antibiotic Selection for Recurrent Urinary Tract Infections in Older Women. *Urology* **2018**, *113*, 26−33.

(7) Cek, M.; Tandoğdu, Z.; Wagenlehner, F.; Tenke, P.; Naber, K.; Bjerklund-Johansen, T. E. Healthcare-Associated Urinary Tract Infections in Hospitalized Urological Patients—a Global Perspective: Results from the GPIU Studies 2003−2010. *World J. Urol.* **2014**, *32*, 1587−1594.

(8) Cassini, A.; Plachouras, D.; Eckmanns, T.; Abu Sin, M.; Blank, H. P.; Ducomble, T.; Haller, S.; Harder, T.; Klingeberg, A.; Sixtensson, M.; Velasco, E.; Weiß, B.; Kramarz, P.; Monnet, D. L.; Kretzschmar, M. E.; Suetens, C. Burden of Six Healthcare-Associated Infections on European Population Health: Estimating Incidence-Based Disability-Adjusted Life Years through a Population Prevalence-Based Modelling Study. *PLoS Med.* **2016**, *13*, No. e1002150.

(9) Renard, J.; Ballarini, S.; Mascarenhas, T.; Zahran, M.; Quimper, E.; Choucair, J.; Iselin, C. E. Recurrent Lower Urinary Tract Infections Have a Detrimental Effect on Patient Quality of Life: A Prospective, Observational Study. *Infect. Dis. Ther.* **2015**, *18*, 125−135.

(10) National Institute for Health and Clinical Excellence. Urinary Tract Infection (Recurrent): Antimicrobial Prescribing NICE Guideline, 2018.

(11) Taylor, R. A.; Moore, C. L.; Cheung, K. H.; Brandt, C. Predicting Urinary Tract Infections in the Emergency Department with Machine Learning. *PLoS One* **2018**, *13*, No. e0194085.
(12) Schmiemann, G.; Kniehl, E.; Gebhardt, K.; Matejczyk, M. M.; Hummers-Pradier, E. Diagnose Des Harnwegsinfekts: Eine Systematische Übersicht. *Dtsch. Arztebl.* **2010**, *107*, 361−367.
(13) McIsaac, W. J.; Hunchak, C. L. Overestimation Error and Unnecessary Antibiotic Prescriptions for Acute Cystitis in Adult Women. *Med. Decis. Making* **2011**, *31*, 405−411.
(14) Tomas, M. E.; Getman, D.; Donskey, C. J.; Hecker, M. T. Overdiagnosis of Urinary Tract Infection and Underdiagnosis of Sexually Transmitted Infection in Adult Women Presenting to an Emergency Department. *J. Clin. Microbiol.* **2015**, *53*, 2686−2692.
(15) Woodford, H. J.; George, J. Diagnosis and Management of Urinary Tract Infection in Hospitalized Older People. *J. Am. Geriatr. Soc.* **2009**, *57*, 107−114.
(16) Cortes-Penfield, N. W.; Trautner, B. W.; Jump, R. L. P. Urinary Tract Infection and Asymptomatic Bacteriuria in Older Adults. *Infect. Dis. Clin. North Am.* **2017**, *31*, 673−688.
(17) Hooton, T. M.; Roberts, P. L.; Cox, M. E.; Stapleton, A. E. Voided Midstream Urine Culture and Acute Cystitis in Premenopausal Women. *N. Engl. J. Med.* **2013**, *369*, 1883−1891.
(18) Bonkat, G.; Pickard, R.; Bartoletti, R.; Bruyere, F.; Geerlings, S.; Wagenlehner, F.; Wullt, B.. *Guidelines on Urological Infections*; European Association of Urology, 2017.
(19) Lehmann, L. E.; Hauser, S.; Malinka, T.; Klaschik, S.; Weber, S. U.; Schewe, J. C.; Stüber, F.; Book, M. Rapid Qualitative Urinary Tract Infection Pathogen Identification by Septifast Real-Time PCR. *PLoS One* **2011**, *6*, No. e17146.
(20) Mach, K. E.; Wong, P. K.; Liao, J. C. Biosensor Diagnosis of Urinary Tract Infections: A Path to Better Treatment? *Trends Pharmacol. Sci.* **2011**, *32*, 330−336.
(21) Holm, A.; Cordoba, G.; Sørensen, T. M.; Jessen, L. R.; Siersma, V.; Bjerrum, L. Point of Care Susceptibility Testing in Primary Care - Does It Lead to a More Appropriate Prescription of Antibiotics in Patients with Uncomplicated Urinary Tract Infections? Protocol for a Randomized Controlled Trial. *BMC Fam. Pract.* **2015**, *16*, No. 106.
(22) Schot, M. J. C.; Van Delft, S.; Kooijman-Buiting, A. M. J.; De Wit, N. J.; Hopstaken, R. M. Analytical Performance, Agreement and User-Friendliness of Six Point-of-Care Testing Urine Analysers for Urinary Tract Infection in General Practice. *BMJ Open* **2015**, *5*, No. e006857.
(23) Ebrahimzadeh, T.; Kuprasertkul, A.; Neugent, M. L.; Lutz, K. C.; Fuentes, J. L.; Gadhvi, J.; Khan, F.; Zhang, C.; Sharon, B. M.; Orth, K.; Li, Q.; Zimmern, P. E.; De Nisco, N. J. Urinary Prostaglandin E2 as a Biomarker for Recurrent UTI in Postmenopausal Women. *Life Sci. Alliance* **2021**, *4*, No. e202000948.
(24) Ricciotti, E.; Fitzgerald, G. A. Prostaglandins and Inflammation. *Arterioscler. Thromb. Vasc. Biol.* **2011**, *31*, 986−1000.
(25) Hannan, T. J.; Roberts, P. L.; Riehl, T. E.; van der Post, S.; Binkley, J. M.; Schwartz, D. J.; Miyoshi, H.; Mack, M.; Schwendener, R. A.; Hooton, T. M.; Stappenbeck, T. S.; Hansson, G. C.; Stenson, W. F.; Colonna, M.; Stapleton, A. E.; Hultgren, S. J. Inhibition of Cyclooxygenase-2 Prevents Chronic and Recurrent Cystitis. *EBioMedicine* **2014**, *1*, 46−57.
(26) Ganguly, A.; Ebrahimzadeh, T.; Zimmern, P. E.; De Nisco, N. J.; Prasad, S. Label Free, Lateral Flow Prostaglandin E2 Electrochemical Immunosensor for Urinary Tract Infection Diagnosis. *Chemosensors* **2021**, *9*, No. 271.
(27) Grieshaber, D.; MacKenzie, R.; Vörös, J.; Reimhult, E. Electrochemical Biosensors - Sensor Principles and Architectures. *Sensors* **2008**, *8*, 1400−1458.
(28) Ganguly, A.; Prasad, S. Passively Addressable Ultra-Low Volume Sweat Chloride Sensor. *Sensors* **2019**, *19*, No. 4590.
(29) Ganguly, A.; Lin, K. C.; Muthukumar, S.; Prasad, S. Autonomous, Real-Time Monitoring Electrochemical Aptasensor for Circadian Tracking of Cortisol Hormone in Sub-Microliter Volumes of Passively Eluted Human Sweat. *ACS Sens.* **2021**, *6*, 63−72.
(30) Sarigul, N.; Korkmaz, F.; Kurultak, İ. A New Artificial Urine Protocol to Better Imitate Human Urine. *Sci. Rep.* **2019**, *9*, No. 20159.
(31) Ganguly, A.; Rice, P.; Lin, K. C.; Muthukumar, S.; Prasad, S. A Combinatorial Electrochemical Biosensor for Sweat Biomarker Benchmarking. *SLAS Technol.* **2020**, 25−32.
(32) Worcester, E. M.; Bergsland, K. J.; Gillen, D. L.; Coe, F. L. Mechanism for Higher Urine PH in Normal Women Compared with Men. *Am. J. Physiol. Renal Physiol.* **2018**, *314*, F623−F629.
(33) Malvern Instruments. Zeta Potential: An Introduction in 30 Minutes, *Zetasizer Nano Serles Technical Note. MRK654-01*, 2011.
(34) Munje, R. D.; Muthukumar, S.; Prasad, S. Lancet-Free and Label-Free Diagnostics of Glucose in Sweat Using Zinc Oxide Based Flexible Bioelectronics. *Sens. Actuators, B* **2017**, *238*, 482−490.
(35) Zorea, J.; Shukla, R. P.; Elkabets, M.; Ben-Yoav, H. Probing Antibody Surface Density and Analyte Antigen Incubation Time as Dominant Parameters Influencing the Antibody-Antigen Recognition Events of a Non-Faradaic and Diffusion-Restricted Electrochemical Immunosensor. *Anal. Bioanal. Chem.* **2020**, *412*, 1709−1717.
(36) Shanmugam, N. R.; Muthukumar, S.; Selvam, A. P.; Prasad, S. Electrochemical Nanostructured ZnO Biosensor for Ultrasensitive Detection of Cardiac Troponin-T. *Nanomedicine* **2016**, *11*, 1345−1358.
(37) Randviir, E. P.; Banks, C. E. Electrochemical Impedance Spectroscopy: An Overview of Bioanalytical Applications. *Anal. Methods* **2013**, *5*, 1098−1115.
(38) Llorella, A.; Navarro-Segarra, M.; Merino-Jiménez, I.; Esquivel, J. P.; Sabaté, N. Electro-Fluidic Timer for Event Control in Paper-Based Devices. *Microfluid. Nanofluid.* **2019**, *24*, No. 10.
(39) Merino-Jimenez, I.; Llorella, A.; Navarro-Segarra, M.; Agramunt, J.; Grandas, A.; Minteer, S. D.; Esquivel, J. P.; Sabaté, N. A Self-Powered Minimalistic Glucometer: A Lean Approach to Sustainable Single-Use Point-of-Care Devices. *Adv. Mater. Technol.* **2021**, *6*, No. 2001051.
(40) Bard, A. J.; Faulkner, L. R. *Electrochemical Methods Fundamentals and Applications*, 2nd ed.; John Wiley & Sons: New Jersey, 2001.
(41) Shanmugam, N. R.; Muthukumar, S.; Prasad, S. Ultrasensitive and Low-Volume Point-of-Care Diagnostics on Flexible Strips-a Study with Cardiac Troponin Biomarkers. *Sci. Rep.* **2016**, *6*, No. 33423.
(42) Shanmugam, N. R.; Muthukumar, S.; Selvam, A. P.; Prasad, S. Electrochemical Nanostructured ZnO Biosensor for Ultrasensitive Detection of Cardiac Troponin-T. *Nanomedicine* **2016**, *11*, 1345−1348.
(43) Pan, Y.; Sonn, G. A.; Sin, M. L. Y.; Mach, K. E.; Shih, M. C.; Gau, V.; Wong, P. K.; Liao, J. C. Electrochemical Immunosensor Detection of Urinary Lactoferrin in Clinical Samples for Urinary Tract Infection Diagnosis. *Biosens. Bioelectron.* **2010**, *26*, 649−654.
(44) Ates, H. C.; et al. Integrated Devices for Non-Invasive Diagnostics. *Adv. Funct. Mater.* **2021**, *31*, No. 2010388.
(45) Sze, A.; Erickson, D.; Ren, L.; Li, D. Zeta-Potential Measurement Using the Smoluchowski Equation and the Slope of the Current-Time Relationship in Electroosmotic Flow. *J. Colloid Interface Sci.* **2003**, *261*, 402−410.
(46) Jagannath, B.; Muthukumar, S.; Prasad, S. Electrical Double Layer Modulation of Hybrid Room Temperature Ionic Liquid/Aqueous Buffer Interface for Enhanced Sweat Based Biosensing. *Anal. Chim. Acta* **2018**, *1016*, 29−39.
(47) Stetefeld, J.; McKenna, S. A.; Patel, T. R. Dynamic Light Scattering: A Practical Guide and Applications in Biomedical Sciences. *Biophys. Rev.* **2016**, *8*, 409−427.
(48) Daniels, J. S.; Pourmand, N. Label-Free Impedance Biosensors: Opportunities and Challenges. *Electroanalysis* **2007**, *19*, 1239−1257.
(49) Pänke, O.; Balkenhohl, T.; Kafka, J.; Schäfer, D.; Lisdat, F. Impedance Spectroscopy and Biosensing. *Adv. Biochem. Eng. Biotechnol.* **2007**, *109*, 195−237.
(50) Scholz, F. et al. *Electroanalytical Methods Guide to Experiments and Applications*, 2nd ed.; Springer, 2010.
(51) Carey, R.; Anderson, F.; George, H.; Hartmann, A.; Janzen, V.; Kallner, A.; Levine, J.; Schiffgens, J.; Srinivasan, A.; Tholen, D. User

Verification of Performance for Precision and Trueness; Approved Guideline − Second Edition, CLSI Document EP15-A2, 2006.
(52) Tholen, D. W.; Kallner, A.; Kennedy, J. W.; Krouwer, J. S.; Meier, K. EP5-A2 Evaluation of Precision Performance of Quantitative Measurement Methods; Approved Guideline − Second Edition, 2004.

https://doi.org/10.1021/acssensors.1c01951
ACS Sens. 2022, 7, 186−198